Medical Research Archives

ESMED
European Society of Medicine

OPEN ACCESS

Published: June 30, 2023

Citation: Mayevsky A, 2023. Real Time *In Vivo* Evaluation of Mitochondrial Activity and Brain Functions during Ischemic Stroke , Medical Research Archives, [online] 11(6). https://doi.org/10.18103/mra.v11i6.3967

DOI
https://doi.org/10.18103/mra.v11i6.3967

ISSN: 2375-1924

RESEARCH ARTICLE

Real Time *In Vivo* Evaluation of Mitochondrial Activity and Brain Functions during Ischemic Stroke

Avraham Mayevsky

The Mina & Everard Goodman Faculty of Life Sciences and the Leslie and Susan Gonda Multidisciplinary Brain Research Center, Bar-Ilan University, Ramat-Gan 5290002, Israel

***Correspondence:** mayevskya@gmail.com

ABSTRACT

More than 50% of total energy consumed by the brain is utilized by active transport processes which are responsible for keeping the ionic homeostasis in the brain. Under an ischemic condition, energy availability is limited, and, as a result, inhibition of the ion pumps is unavoidable. The initial consequence of such inhibition is a gradual accumulation of K^+ in the extracellular space leading to a second phase of the ischemic depolarization phenomenon. During ischemic depolarization, extracellular K^+ will increase 15-20-fold, while extracellular Ca^{2+} is decreasing 10 fold. Another optional effect of mild ischemia is the development of Cortical Spreading Depression due to the leakage of K^+ into the extracellular space. The Mongolian gerbil provides a very useful animal model to study the effects of ischemia on brain functions.

The aims of the study were as follows: (1) To elucidate the mechanism behind the development of ischemic depolarization or cortical spreading depression under unilateral and bilateral carotid artery occlusion. (2) To correlate the kinetics of the recovery processes to the level of ischemia.

We tested the correlation between energy depletion level (evaluated by intramitochondrial NADH redox state and Cerebral Blood Flow) and the development of ischemic depolarization or cortical spreading depression (evaluated by extracellular K^+, H^+, Ca^{2+}, DC potential and 366 nm reflectance changes) under partial and complete ischemia using the multiparametric monitoring system.

The results could be summarized as follows: (1) Under bilateral occlusion, in all gerbils the ischemic depolarization was recorded within 1-2 min. (2) Under unilateral occlusion, the level of ischemia obtained was significantly smaller and led to the ischemic depolarization in about 60% of the gerbils. (3) The K^+ leakage during the ischemic depolarization had an 'all or none' nature in terms of maximal K^+ levels and time to reach it. (4) The main effect of various lengths of bilateral occlusion was on the recovery time of extracellular K^+ level. (5) Cortical spreading depression develop in most cases during the recovery from the ischemic event when ischemic depolarization was not recorded under the ischemic episode.

Introduction

The initial event that leads to the occurrence of Stroke is a sudden disturbance in microcirculatory blood flow and a drop in oxygen supply to the brain tissue. Due to the lack of oxygen, mitochondrial dysfunction is developed and the production of ATP - the energy source of all brain physiological activities will be inhibited. During a stroke event there are changes that take place in the short time scale (seconds to few minutes) followed by long term events that may lead to irreversible damage to the tissue. In our previous studies we investigated the effect of brain ischemia and cortical spreading depression (Fig. 1 parts 9 and 10) on mitochondrial functions (NADH redox state, part C in Fig. 1) as well as other pathophysiological events developed in the brain.

Figure 1 demonstrates the main elements that build a typical human (A) cerebral tissue (B). The cellular compartment is typical neurons and glial cells as well as the synapses. The small blood vessels – the arterioles and the capillaries, provide the oxygen and other nutrients. A few of the main events developed during ischemia were selected and shown in the right column. Under ischemia, the primary event is the decrease in CBF (1) and microcirculatory hemoglobin oxygenation (2). Therefore, the oxygen delivery (3) to the brain decreased and is detected as an increase in the intramitochondrial NADH (4). The next step is the inhibition of the ion pumps such as the Na^+ K^+ ATPase due to the low levels of ATP in the cell (5). The accumulation of K^+ in the extracellular space (6) and the increase in in the intracellular calcium (7) will be recorded. The last event (8) is the decreased spontaneous electrical activity (ECoG) and the ischemic depolarization phase of the brain tissue. This situation will persist until reperfusion is started and normal CBF is established. The treatment of patients after the development of brain Ischemic event - Stroke is a significant unsolvable challenge to clinicians as well as to brain research scientists. One of the main reasons leading to this situation is the multifactorial nature of this brain pathological event leading to very high mortality as well as permanent irreversible damages to brain activities.

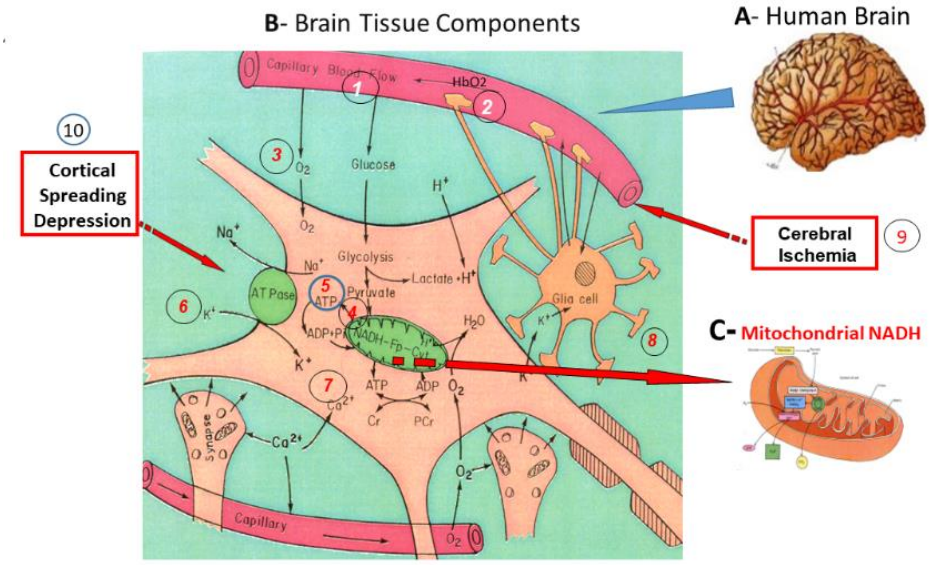

Figure 1: Schematic presentation of the "basic building stones" of a typical cerebral cortex tissue (B) of the human brain (A). In the current paper two pathological states will be discussed namely, cerebral ischemia (9) and cortical spreading depression (10). (modified [1]).

Brain Energy Metabolism

It is well established that normal brain activities depend on the continuous supply of oxygen due to the high O_2 consumption (about 20% of the total O_2 used by the body) and due to the very limited reserve of dissolved O_2 in the brain tissue. It is possible to assess this ability through the knowledge of changes in the oxygen balance, i.e. the ratio of oxygen supply to oxygen demand in the tissue. This concept was suggested by Barcroft about 110 years ago [2]. He described the relationship between tissue activity, oxygen consumption and increase in blood supply as a compensation mechanism. Actually, Barcroft, was the first scientist that described the concept of "Tissue Oxygen Balance". Schematic presentation of the balance between oxygen supply and demand in a typical tissue is shown in Figure 2. The supply of oxygen is

dependent upon microcirculatory blood flow (TBF), blood volume (TBV) and the level of oxygen bound to the hemoglobin (HbO_2) in the small blood vessels, namely, in the microcirculation. The level of microcirculatory oxygenated hemoglobin or the tissue pO_2 is affected by two factors, namely, oxygen consumption by the mitochondria and the microcirculatory blood flow and volume. The demand for oxygen is affected by the specific activities taking place in the brain as seen in the right side of Figure 2. The intracellular level of mitochondrial NADH (the reduced form) is a parameter related to oxygen balance as seen in the center part of the figure. Stroke may develop when the supply of oxygen is decreased while the demand is initially continuing at the same rate. All cells in the body including the brain depend on a continuous supply of ATP (adenosine tri-phosphate) in order to perform their different physiological and biochemical activities shown in the right side of Figure 2.

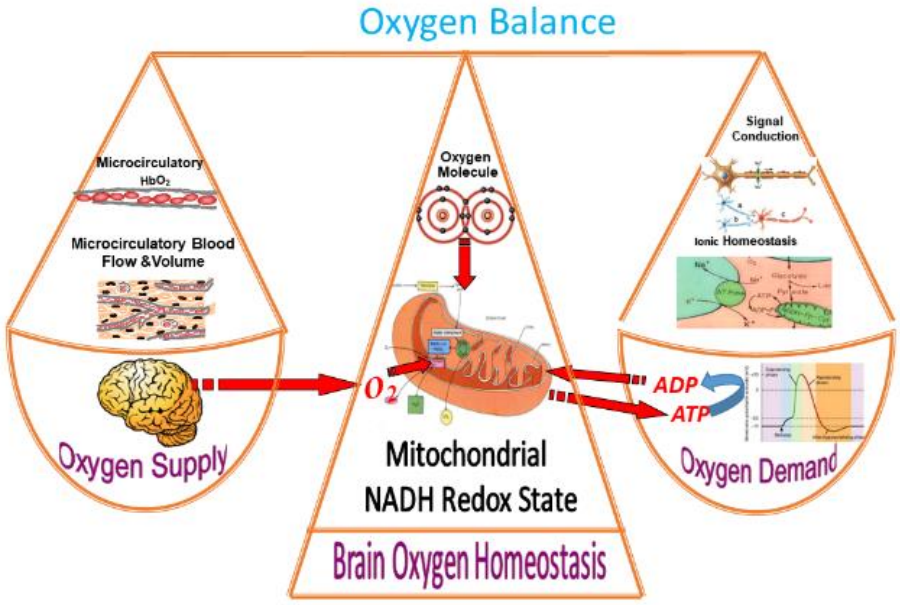

Figure 2: Brain oxygen balance evaluated by oxygen supply and demand. Oxygen supply could be evaluated by monitoring brain blood flow (CBF), brain blood volume (CBV), hemoglobin oxygenation (HbO_2) and brain tissue oxygen partial pressure. Oxygen demand includes Ionic Homeostasis, Signal Conduction and Biochemical synthesis. Mitochondrial NADH redox state serve as an indicator for brain oxygen balance (modified [1]).

The continuous supply of oxygen to the mitochondria depends on two microcirculatory parameters: tissue blood flow (TBF) in the diffusible small vessels (small arterioles and capillaries), and the level of hemoglobin oxygenation or saturation (HbO_2) in the small vessels. Any change in the oxygen consumption by the mitochondria will be compensated either by downloading the extra oxygen needed from oxygenated hemoglobin or via an increase in the blood flow. Under a restriction of oxygen supply (i.e ischemia), mitochondrial function will be inhibited and ATP production will decrease, while glycolysis will become stimulated. Mitochondrial dysfunction is involved in the pathologies of the nervous system, such as traumatic brain injury [3,4], spinal cord injury [5] and stroke [6]. The role of NADH in cellular function and cell death as well as in brain functions, diseases and aging were reviewed in 2006 [7,8]. The connection between mitochondria and neuronal activity was described in detail in 2007 [9]. In 2013 Edeas and Weissig published a paper claiming that the future of medicine will come through mitochondria [10]. The possibility of monitoring mitochondrial function *in vivo*, in experimental animals and patients is of great importance and could contribute significantly to the understanding of various pathological processes. Most of the information on mitochondrial function has been accumulated from *in vitro* studies. A relatively small portion of published papers dealt with the monitoring of mitochondrial function *in vivo* and in real-time. During the past 50 years, we have published over 150 papers in this very significant

area, including the largest number of studies using NADH redox state monitoring in patients as well.

Monitoring of NADH: From Isolated Mitochondria to Brain *In Vivo*

The need for an intracellular pO_2 indicator, as a physiological and biochemical parameter of living tissue, has emerged over 60 years ago [11]. Mitochondria are the intracellular organelles that consume most of the oxygen consumed by the entire body. Therefore, the redox state of electron carriers in isolated mitochondria *in vitro* as well as *in vivo* as a function of oxygen concentration has been extensively studied. Chance et al. concluded that "For a system at equilibrium, NADH is at the extreme low potential end of the chain, and this may be the oxygen indicator of choice in mitochondria and tissue as well" [12]. Lubbers in 1995 concluded that "the most important intrinsic luminescence indicator is NADH, an enzyme of which the reaction is connected with tissue respiration and energy metabolism" [13]. The pioneer work of Chance, Williams, Connelly and other collaborators, in the early 1950's, opened up new possibilities enabling the study of mitochondrial function *in vitro*, and later on *in vivo* monitoring became a reality [14-17]. The shift from studying mitochondrial NADH redox state in isolated mitochondria to higher cellular and tissue organization levels started in the late 1950's [18]. The main breakthrough occurred in 1962, a year that at least 6 papers described the *in vivo* monitoring of various organs in the anesthetized rat [11,19-23]. The crucial issue is: Can we extrapolate from the results obtained in monitoring of mitochondrial NADH *in vitro* to *in vivo* conditions? Mitochondrial function and its metabolic states under *in vivo* condition are completely different from the definition made for isolated mitochondria by Chance and Williams [15]. The main differences between the two situations presented in Figure 3 left side and Figure 3 right side are as follows:

1. The isolated mitochondria are not inter-connected to other intracellular organelles and components.
2. The amount of oxygen available in the mitochondrial medium is not regulated by changes in blood flow or hemoglobin oxygenation under *in vitro* conditions.
3. One of the largest oxygen or energy consumers i.e. various ions pumps, are missing from the isolated mitochondria preparation.
4. When ADP is added to State 4 mitochondria, ATP will be synthesized but will not be consumed in parallel as occurred under in vivo conditions.
5. The isolated mitochondria preparation is not exposed to systemic changes in hemodynamic and other physiological parameters occurring in the organism.

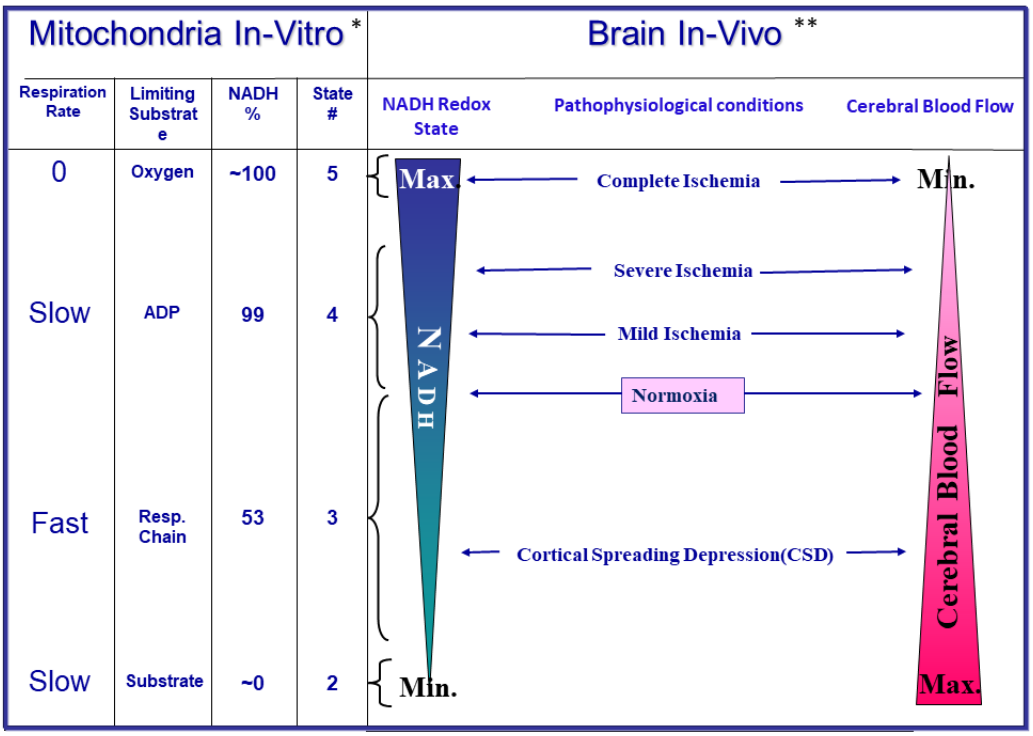

Figure 3: Comparison between mitochondrial metabolic state (*in vitro*), defined by Chance & Williams in 1955 (left side) and responses of the *in vivo* brain to changes in Oxygen supply and demand induced by brain activation described by Mayevsky (right side). (modified [1]).

There is a clear data interpretation dilemma as follows: Can we compare and define the resting state (4) and active state (3) under *in vivo* situations to the *in vitro* definitions? As seen in Figure 3, the maximal NADH level is achieved under complete O_2 deprivation that can be induced both under *in vitro* and *in vivo* conditions. This signifies that this definitive point can be used to determine State *5 in vivo* as well. As can be seen in the Table (Fig. 3), the steady state NADH level at State *4* is 99%, namely that most of the NAD is in the reduced form NADH. When the mitochondria are shifted to State 3, by adding ADP, the NADH becomes more oxidized and the NADH level is decreased to 53% of the reduced form. Moving from State 4 to State *5*, and eliminating the oxygen from the media will have a very small effect on the NADH level namely, changing from 99% to 100%. It is important to note that other members of the respiratory chain behave somewhat similarly to the NADH. When the mitochondria are shifted to State 2, NADH level is 0 since the NAD is the dominant state in the absence of a substrate. The problem is to determine the 'resting' metabolic state of a tissue in an in vivo situation. If we adopt the *in vitro* value of a resting state (State 4), this would signify that the increase in NADH during State *5*, induced by anoxia (0% O_2), would be only 1% namely from 99% to 100%. According to all in vivo studies, this is not the case, and during anoxia the increase in NADH is much larger than the decrease under State 4 to 3 transition. When we started our monitoring of NADH redox state using fiber optic based fluorometry/reflectometry in 1972, we used the brain *in vivo* exposed to various conditions in real time [24]. We found that the NADH level could either increase or decrease from the baseline level calibrated in the normoxic animal [25]. The initial results were plotted against the perturbation used as shown in the right side of Figure 3. The relative changes in brain NADH under various perturbations as compared to the Chance and Williams definitions (Fig. 3 left side) are presented. Although the maximal level of NADH could be achieved *in vivo* by exposing the animal to anoxia (100% nitrogen), the minimal level that could be monitored *in vivo* is very hard to achieve. We tried to build the scale between maximal and minimal levels of NADH by exposing the brain to many types of perturbations. In the Table, the horizontal lines represent the relative change in NADH recorded during the perturbation. The values are not accurate but rather trying to map the scale of NADH changes. The question is how to locate the *in vivo* scale relative to the *in vitro* definition shown on the left side. According to the changes recorded, it seems that the so-called "resting brain" is not at State 4 (99% NADH) but rather around 3.5-3.6. As seen, NADH will increase by various factors such as various level of ischemia. Under complete ischemia, the NADH will reach its maximal level – State *5*. Activation of the brain by inducing cortical spreading depression led to a very large decrease in NADH. The main issue in the scaling or the responses is how to "push" the brain in vivo to minimal NADH levels. As of now it seems that this question remains open and unsolved. Activation of the brain (cortical spreading depression) under conditions of restricted amounts of oxygen, such as partial ischemia, will lead to an increase in NADH (reduction) instead of a decrease (oxidation) as found in the normoxic brain. Those results found in various experimental conditions led to the dilemma. According to Chance and Williams, ATP production related to State 4 to State 3 transition is always correlated to a decrease or oxidation of NADH from 99% to 53%. The question is how ATP turnover could increase under NADH increase (reduction) and not decrease (oxidation) in the case of brain activation under oxygen restriction. We want to make sure that the experimental results do not represent a technical artifact related to the monitoring itself. We assumed that by using appropriate modeling methods the dilemma could be clarified or resolved [26]. During the years 1972-2014 we were able to monitor brain NADH redox state in many pathophysiological conditions in experimental animals as well as in neurosurgical patients in the OR and in the ICU [27,28].

Effects of Stroke on mitochondrial function

During the last few years, few papers described the interrelation between mitochondrial function and ischemic stroke. The relations between cerebrovascular function and brain bioenergetics after ischemia was investigated by Rutkai et al. [29]. In 2018 Liu et al. [30] reviewed the subject of mitochondrial in ischemic stroke. They discussed the potential use of mitochondrial as therapeutic targets for stroke treatment strategy. Another review was published in 2018 discussing the diverse role of mitochondria in ischemic stroke [31]. Sperling et al. [32] measured respiration *in vitro* of isolated mitochondria in relation to stroke studies. Chen et al. [33] used mitochondrial transfer as a therapeutic strategy against ischemic stroke. Very recently, mitochondrial quality control in stroke was suggested and published [34-36].

The aim of the present study is to demonstrate the effects of various durations of brain partial or complete ischemia on the mitochondrial NADH

redox state as well as other brain functions recorded in real time.

Methods

The development of UV light transmitting optical fibers at the beginning of the 1970's enabled us the measurements of mitochondrial NADH redox state *in vivo* using the brain of small animals. Later on additional parameters were added to the monitoring system that enabled us to use a brain physiological mapping system as presented in Figure 4. Typical monitoring systems are presented in Figures 5 and 6.

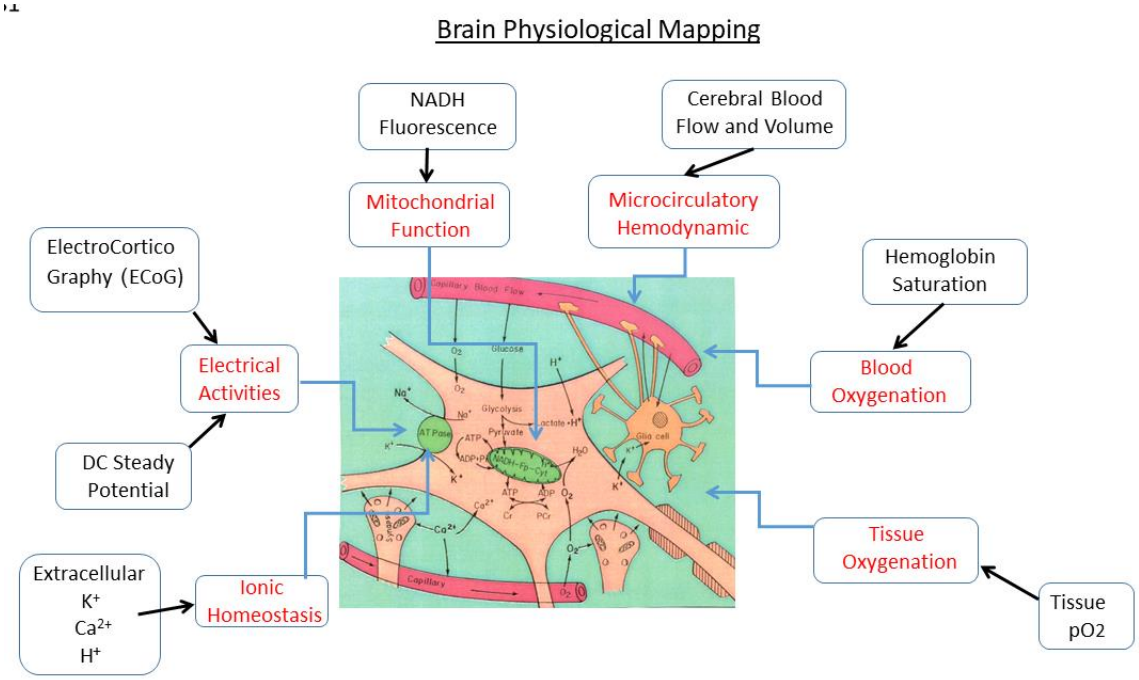

Figure 4: Schematic presentation of the concept "Brain Physiological Mapping". All techniques that are presented were developed and used in our laboratory (see text for details). (modified [1]).

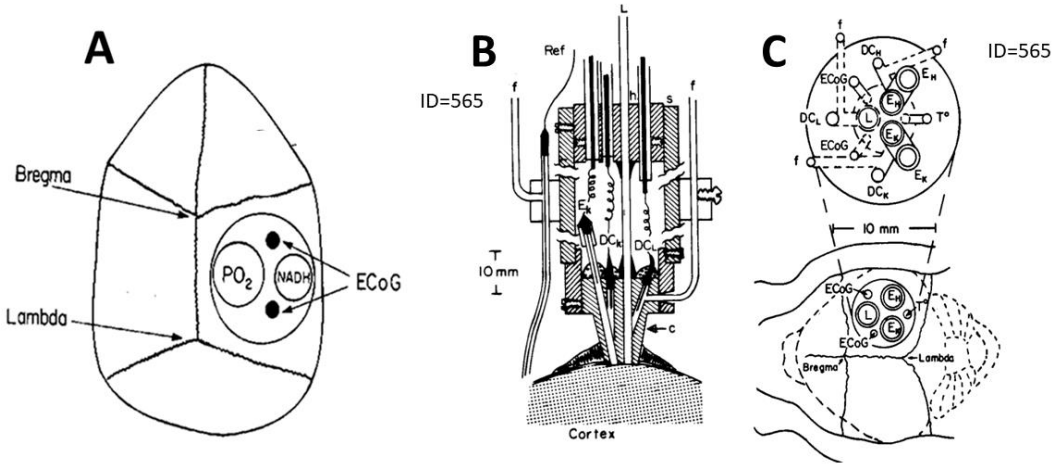

Figure 5: **A** - Schematic presentation of the various probes location above the brain of the gerbil. The large cannula contained the light guide for NADH measurement, the PO_2 and ECoG electrodes [37]. **B** - The Multiprobe cross section of wide end of the MPA cannula [38].

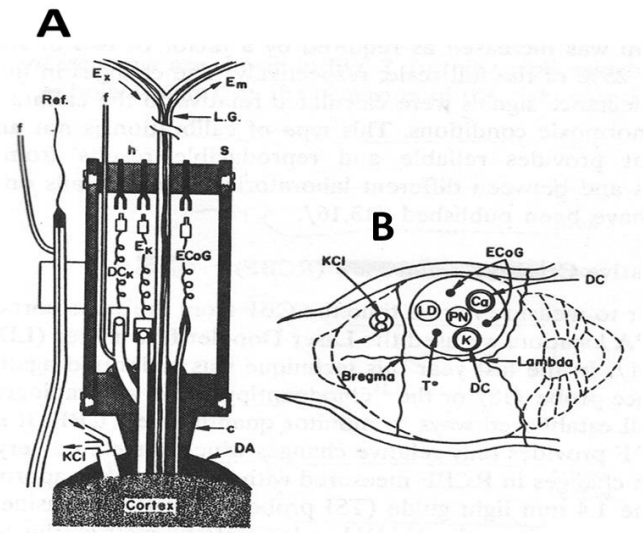

Figure 6: Schematic representation of the Updated multiprobe assembly (MPA) in a longitudinal section as well as its location on the gerbil brain. L.G.- light guide, c - cannula, f - filling tube for the DC and reference electrodes, h - connector holder, s - plexiglass sleeve, DA-dental acrylic, T° - temperature Probe, Ex - excitation, Em - emission, KCl - push pull cannula to elicit CSD, ECoG - electrocortical electrodes, PN - NADH monitoring light guide, LD - Laser Doppler flow meter light guide [39].

Mitochondrial NADH Redox State Fluorometry

NADH monitoring from the brain surface is performed by the fluorometric technique based on the original work by Chance and Williams presented in detail [11,24,40]. The excitation light (366 nm) is passed from the fluorometer to the tissue through a bundle of quartz optical fibers. The emitted light (450 nm), together with the reflected light at the excitation wavelength, is transferred to the fluorometer through another bundle of fibers. The measured changes in fluorescence and reflectance signals are calculated as percent values relative to the calibrated signals under normoxic conditions. This type of calibration is not absolute, but it provides reliable and reproducible results for different animals and different laboratories [25,41].

Microcirculatory Blood Flow (TBF)

To measure in real time, the TBF from the same cortical area as the MPA location, we used the Laser Doppler flowmeter (LDF) technique [42-44]. The LDF measures relative flow changes, and readings have been shown to correlate with the relative changes in cerebral blood flow-CBF measured by the two other quantitative approaches (for a review see [44]) The principle of the LDF is to utilize the Doppler shift, namely, the frequency change that light undergoes when reflected by moving red blood cells. A beam of low-power or diode laser light is transmitted by an optical fiber to the tissue. After the multiple scattering of the light, another optical fiber picks up the reflected light that is recorded by a photo detector. The run signal is analyzed by a complicated algorithm developed by the manufacturers, and the results are presented in percentage of a full scale (0-100%), thereby providing arbitrary relative flow values. To quantify and normalize CBF values, we defined the reading value after death as 0 CBF. The 100% value was defined as percent CBF read on the LDF scale during the control period.

Hemoglobin Oxygenation

The level of oxygenated hemoglobin can be monitored at the microcirculatory level using the absorption spectrum of hemoglobin, which is different in its oxygenated or deoxygenated state. The tissue surface is illuminated with 585 nm light which is an isosbestic point, and with 577 nm light, which is a non-isosbestic point, in which the oxy-hemoglobin absorb more light than the deoxyhemoglobin form. By subtracting the 585 nm reflectance from the 577 nm reflectance, a parameter correlated to blood oxygenation is obtained. A detector collects the light reflected from the tissue and converts it into oxy-hemoglobin levels [45-47].

Ion-Selective Electrodes and DC Potential

To monitor the extracellular levels of K^+, Ca^{2+} and H^+, we used specially designed mini electrodes made by World Precision Instruments (WPI;

Sarasota, FL). A flexible tubing made of polyvinyl chloride was sealed at one end with a membrane sensitive to a specific ion. The tube was filled with the appropriate solution and connected to an electrode holder with a salt bridge between the membrane and an Ag-AgCl pellet located inside the holder. The interface between the polyvinyl chloride tubing and the holder was glued with epoxy, and such electrodes were usable for a few weeks. The sensitivity of the electrodes to the specific ion was close to the Nernstian value, namely, 50-60 mV/decade for K^+ and H^+ or 25-30 mV/decade for Ca^{2+}. DC potential was measured concentrically around the ion selective electrodes. Each electrode had a saline bath around its perimeter, and an Ag-AgCl electrode (WPI, USA) was connected to it (for more details see ref. [38,48,49].

Reference Electrode

An Ag-AgCl electrode connected via a saline bridge to the neck area of the animal was used as the reference electrode. Polyethylene tubing stuffed with a cotton string that expanded when wet was inserted into the electrode holder (WPI) and glued with 5-min epoxy [38].

ElectroCorticoGraphy-ECoG

Spontaneous electrical activity of the brain surface was measured by two polished stainless steel rods or silver wire inserted into the MPA [38].

Multiprobe Assembly (MPA)

The classical MPA includes optical fibers for the monitoring of mitochondrial NADH redox state by the fluorometric technique, optical fibers for the monitoring of microcirculatory blood flow by laser Doppler flowmetry, one or more selective mini-electrodes for the monitoring of extracellular K^+, H^+ or Ca^{2+} levels, each surrounded by a DC electrode, two needle electrodes for EEG monitoring, a thermistor for the cortical temperature monitoring, and in some cases an ICP (intracranial pressure) probe (Camino Laboratories, San Diego, CA, USA). Our "classical" MPA system presented in Figures 5 and 6 were described in much details in our previous publications [50-53].

Surgical procedures

Animals: Our experiments were performed on adult male Wistar rats (200-300 gr.) and Mongolian gerbils (50-70 gr.) according to the NIH guidelines for the care and use of laboratory animals, and after the approval of the Institutional Animal Care authorities.

Surgical Preparations

The animals were anesthetized by an IP injection (0.3 ml/100 g) of Equithesin (E-th) (each ml contains: pentobarbital 9.72 mg, chloral hydrate 42.51 mg, magnesium sulfate 21.25 mg, propylene glycol 44.34% w/v, alcohol 11.5% and water). We have been using this anesthetic for approximately 30 years and it has never shown significant effects on mitochondrial activity. For drug administration, Polyethylene catheters are introduced into the femoral vein and, for the measurements of arterial blood pressure and blood sampling, the femoral artery is cannulated.

Preparations for brain monitoring

The animal is placed on the operation table and the mouth is fixated in a special holder. A midline incision is made in the head of the animal and the skull is exposed. An appropriate hole is drilled in the parietal bone for the light guide holder or the MPA probe and four screws are drilled into the skull, for a better fixation of the monitoring device to the cerebral cortex with dental acrylic cement. In cases of extracellular ions monitoring, the Dura mater is gently removed. Then, the monitoring probe is placed on the cerebral cortex, using a micromanipulator to avoid extra pressure on the cerebral tissue, and the probe is fixed in position using dental acrylic cement. When monitoring anesthetized animals, additional injections of anesthetic (E-th) are given to the rats or gerbils at 30 minutes' intervals during the monitoring (0.1 ml Equithesin/100 gr. body weight). On the other hand, in protocols requiring awake animals (usually rats) the animal is placed in a special cage with an upper window that enables real time monitoring of the brain during the experimental period.

The Global ischemia model

Before craniotomy, the animal is placed on its back and a midline section is made in the neck, exposing the carotid arteries and isolating them from the Vagus nerves. Thereafter, a 4-0 silk suture is placed around the arteries and prepared for later ligation. In the chronic ischemia model, after artery occlusion, the incision in the animal's neck is closed and the animal is returned to the cage. The monitoring is preformed 24 hours later.

Results

1. **Monitoring of NADH during acute and chronic brain ischemia.**

After the development of the fiber optic surface fluorometry [24,25] we tested the effects of partial brain ischemia (ligation of the two carotid arteries)

in rats on the responses to brain activation induced by cortical spreading depression(CSD) [54].

The protocol of the experiment in this part was the following: The rat was anesthetized and operated on as described in Methods, and 30 min after the operation, NADH as well as ECoG measurements started while the rat was anesthetized. During the control period of the experiment the brain was exposed to N_2 for one minute in order to check the metabolic state of the brain. The response of the brain to cortical spreading depression was tested by washing the surface of the dura with KCl solution (0.4-0.6 M) through the push-pull cannula. After control values were obtained and when the rat was awake the two carotid arteries were ligated while measuring the NADH and ECoG. At various intervals of time after ligation the brain was exposed to spreading depression and compared to the control values.

Figure 7 shows a typical response of the brain to acute bilateral carotid arteries ligation. Part A shows the response of the NADH to spreading depression and the effect of the ligation on the steady state level of NADH. Parts B, C and D show the response of NADH to spreading depression elicited 15 min, 90 min and 18h, respectively, after the ligation. In this particular animal the changes of the reflectance (upper trace in each part) was minimal during the spreading depression cycles in part A. The effect of the ligation on the oxidation reduction state of NADH was transient, namely, that a small increase was recorded during the ligation, but within two minutes it recovered to the base line. The main effect of the ligation is on the response of the brain to spreading depression which increases oxygen utilization [55-58] During the first 60 min after ligation the oxidation cycle can be detected as a response to CSD, but the amplitude of the oxidation (decrease) was diminished and the duration of the cycle became much longer (almost 4 min in B and only about 2 min in A). The qualitative change in the response of the brain to CSD started several hours after the ligation. In part C one can see the response to CSD 90 min after the ligation. The corrected NADH trace, shows a biphasic response of NADH to CSD. At the beginning of the cycle an increase in NADH was recorded, while afterwards the NADH decreased below the base line level. In part D (18h after ligation) the response of the brain was completely opposite to what was measured before the ligation (part A). It seems that instead of an 'oxidation cycle' as a response to CSD, we found a 'reduction cycle'. In this animal the correction of the NADH for hemodynamic changes is not necessary and the uncorrected trace also shows the same results.

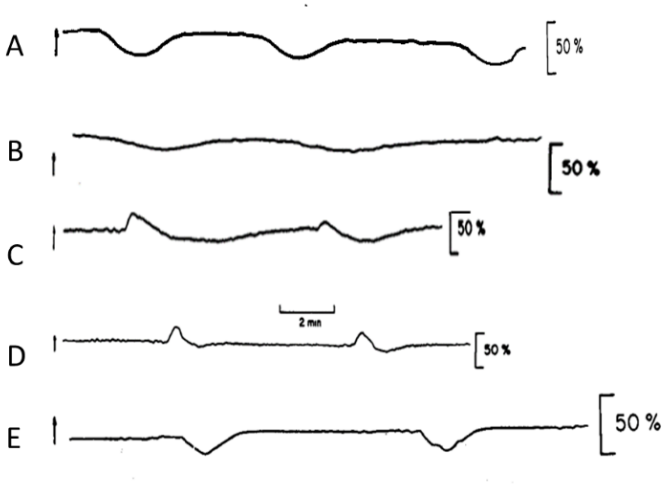

Figure 7: The effect of acute and chronic bilateral carotids occlusion on the metabolic response (NADH redox state) to cortical spreading depression (CSD). Part A shows the response to CSD before the occlusion. Parts B, C and D were measured 15 min, 90 min and 18h after occlusion, respectively. Part E was measured 10 days after the bilateral chronic carotid arteries ligation [54].

The effects of chronic bilateral carotid occlusion were performed as well. In this set of experiments, the occlusion of the two carotids was done at different time intervals before the NADH and ECoG were measured. The various animals ranged between 15h and 14 days of carotid occlusion. After operation and implantation of the light guide holder and ECoG electrodes, the rat was connected to the fluorometer. In order to test the effects of the chronic occlusion, the brain was exposed to CSD elicited by washing KCl solution epidurally. According to the results we divided the rats into

three groups: (1) occlusion up to 3 days; (II) occlusion of 4--7 days; (III) occlusion of 8-14 days. The effect of the ligation on the response of the brain to CSD was found to be a reversible effect. In rats of the first group (up to 3 days) the NADH fluorescence showed a 'reduction cycle' after application of KCl epidurally as was measured after acute bilateral ligation (Fig. 7D). In the third group (8-14 days) the response to CSD was as in the normal brain. In the second group (4-7 days) the results were not clear-cut and were seen as dependent upon the physiological and metabolic state of the animal and the brain. Fig. 7E shows the results obtained from the brain after 10 days of bilateral occlusion.

2. The effects of Ischemia on brain oxygen level and mitochondrial function

In the present study we correlated for the first time the changes in NADH fluorescence, changes in the reflected light, and the changes in pO_2 measured with a surface electrode. The interrelation between the three parameters measured was tested under various conditions, such as: CSD, and ischemia. The methodology used in this study seen in Figure 5A was described in details previously [37].

Figure 8 presents the effect of two sessions of ischemia on the oxygen levels in the brain as well as the redox state of mitochondrial NADH measured simultaneously. Figure 8 presents the effects of unilateral or bilateral carotid artery occlusion. In this animal the occlusion of the contralateral carotid (Locc) had a very small effect on the NADH or the pO_2. Occlusion of the right carotid (while the left one was closed) induced a large fall in pO_2 and an increase of NADH with a similar kinetics. The recovery after bilateral recirculation was fast, without any significant overshoot in the pO_2. In the second ischemia episode, when N_2 was applied to the ischemic brain, a large overshoot in the pO_2 was recorded after recirculation. Here again the large increase in pO_2 was parallel to the large decrease in reflectance with the same kinetics toward the normoxic level. The NADH shows an oxidation cycle after recirculation due to CSD, as can be seen in the ECoG trace. Figure 8 shows the response of the anesthetized brain to bilateral carotid artery occlusion. During the recovery period the pO_2 returns to its normoxic level and then goes down after nitrogen application together with the large increase in NADH. The conclusion from this study is that the length of the ischemia affects the recovery process from the lack of oxygen. We assumed that the lack of oxygen may lead to internal accumulation of potassium in the extracellular space which could initiate a wave of CSD.

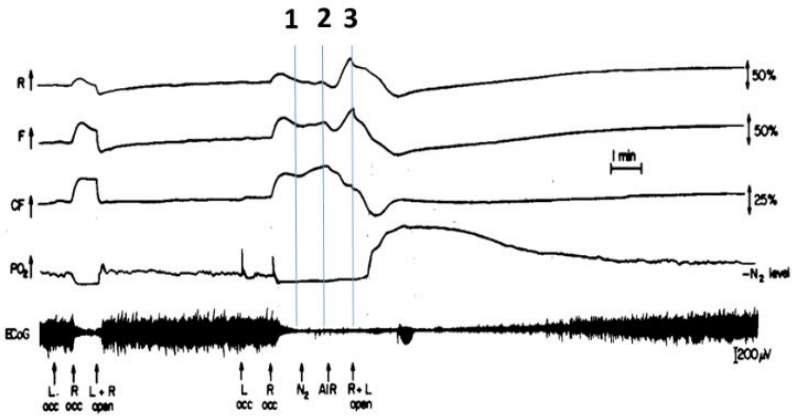

Figure 8: The effects of carotid arteries occlusion on the metabolic and electrical activity of the slightly anesthetized gerbil brain. R, F, CF, reflectance, NADH fluorescence and corrected NADH fluorescence, respectively PO_2, partial pressure of oxygen [37].

3. Responses of NADH, pO_2 and extracellular K^+ to ischemia

The development of ischemic depolarization(ID) is a well-known and documented phenomenon [59-61] but the mechanism behind it is not clear as yet (for review see Hansen [62]). It is not clear what the reason for the change in K^+ leakage during ischemia is. One possibility is that the energy stores depletion reached a critical low level or may be that the level of K^+ in the extracellular space reached a certain point. This hypothesis has not been tested in the gerbil model as yet. In order to shed some light on the question of ID development mechanism we have designed the following study.

In order to study the interrelation between the decrease in pO_2, accumulation of potassium in the

extracellular space and the development of ischemic depolarization after ischemic episode we developed the multiparametric monitoring system presented in Figure 5B and 5C. The specific question we aimed to answer by this study are as follows: (1) is the energy depletion level during the ischemic insult a critical factor in the development of ID (complete loss of ion homeostasis)? (2) What is the effect of Na^+K^+ATPase inhibition level during early ischemia (rate of K^+ leakage) on the development of ID? In order to obtain answers to those questions we performed the following experimental protocol: The effects of two types of ischemic insult, namely, two levels of ischemia (unilateral or bilateral carotid occlusion in gerbils).

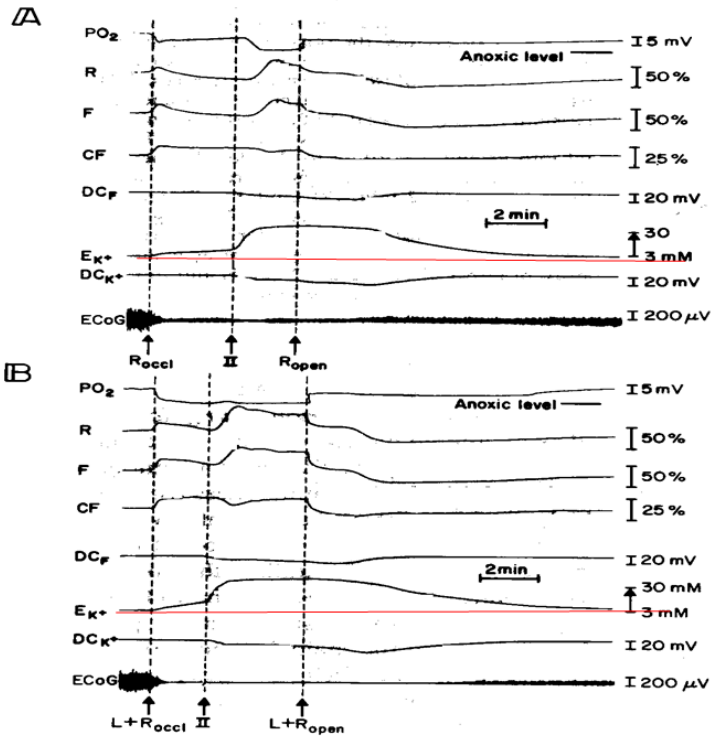

Figure 9: Effects of unilateral (**A**) and bilateral (**B**) carotid artery occlusion on the metabolic, ionic and electrical activities in the gerbil brain. Line II represents the appearance of the ischemic depolarization event, pO_2, partial pressure of oxygen; R, F, CF, reflectance, fluorescence and corrected fluorescence, respectively; DC_F, DC_{K^+}, Direct Current steady potential measured around the light guide and the potassium electrode, respectively; ECoG, ElectroCorticoGram [63].

Under complete or near-complete ischemia (bilateral carotid artery occlusion) a uniform type of response was recorded in all gerbils, as shown in Figure 9B. The initial response was a decrease in energy supply as can be seen by the decrease in pO_2 and an increase in NADH redox state (CF trace). In this gerbil, the pO_2 decreased to almost the anoxic level. It seems that a small posterior communication artery to the basilar artery supplied a small amount of O_2 to the monitored site even under bilateral occlusion. At a certain point (II), ischemic depolarization occurred and led to a change in the slope of the K^+ accumulation and a negative shift in the DC steady potential. The DC negative shift was recorded also near the light guide (DC_F) indicating that the ischemic depolarization is a general event in all cortical areas. As detected by the light guide, a large increase in light reflectance was recorded and affected also the NADH signal but as shown by the pO_2 levels the apparent oxidation of NADH seen in the CF signal is only a transient artifact. When partial ischemia was induced, different type of responses was recorded as seen in Figure 9A, when only the right carotid artery was occluded. The responses shown in Figure 9A are very similar qualitatively to those recorded under bilateral occlusion (Fig. 9B) but with different kinetics (slower) as can be seen by the appearance of line II. The other type of response to unilateral occlusion (figure not shown) has less dramatic effects on the K^+ leakage pattern. After an initial increase, the K^+ reaches a plateau level until the reperfusion time

and the ID response was not recorded in this type of gerbil [63].

4. Development of CSD or ID during or after Brain Ischemia

In few gerbils it was found that even after severe ischemia for 4 minutes, induced by occlusion of the two carotid arteries in the gerbil, for few minutes, ID or CSD was not developed and the brain recovered to its pre-ischemic level of all monitored parameters as seen in Figure 10.

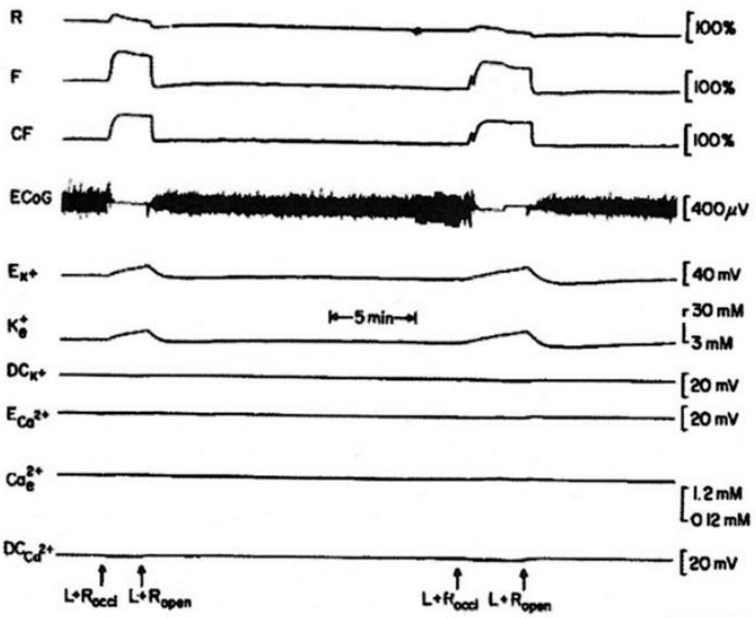

Figure 10: Responses to bilateral carotid arteries occlusion (L + R occl) in the Mongolian gerbil brain. The effects of severe ischemia (different durations) on the metabolic ionic and electrical activities are presented. R, F, CF - Reflectance, fluorescence and corrected fluorescence; ECoG - Electrocorticogram; E_{K+}, K^+_e, ECa^{2+}, Ca^{2+}, Uncorrected and corrected potassium and calcium ion concentrations, respectively; DCK^+, $DCCa^{2+}$ - DC steady potential around the K^+ and Ca^{2+} electrodes [39].

In another gerbil it was found that CSD may developed during the ischemic episode but will be seen as a separate even as seen in Figure 11. In this gerbil the CSD recorded in part B was separated from the ischemic episode. As seen in part A of Figure 11, all parameters and even the ECoG was recovered after the reopening of the 2 carotid arteries.

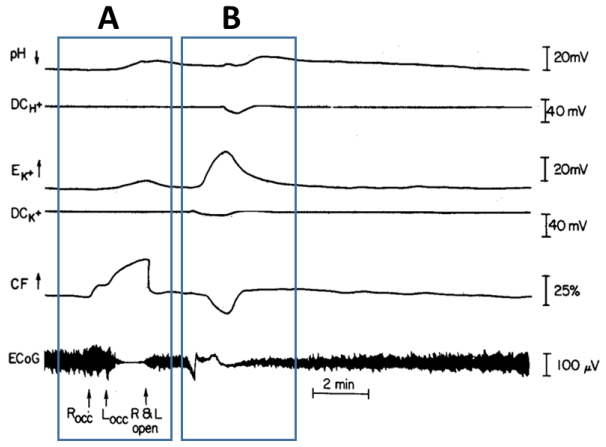

Figure 11: Effects of ischemia (**A**) on metabolic, ionic, and electrical signals measured from a slightly anesthetized gerbil. Spontaneous spreading depression cycle was developed after ischemic episode (**B**). In this experiment we recorded corrected fluorescence alone (CF) without uncorrected fluorescence and reflectance. For abbreviations see text.

Another example is presented in Figure 12. As seen in part A, 2 minutes of ischemia led to changes that recovered immediately after the reopening of the 2 arteries. As seen in part B of Figure 12, a CSD wave was induced by the ischemia, and was recorded at the time of the reperfusion of the brain with blood (L&R open).

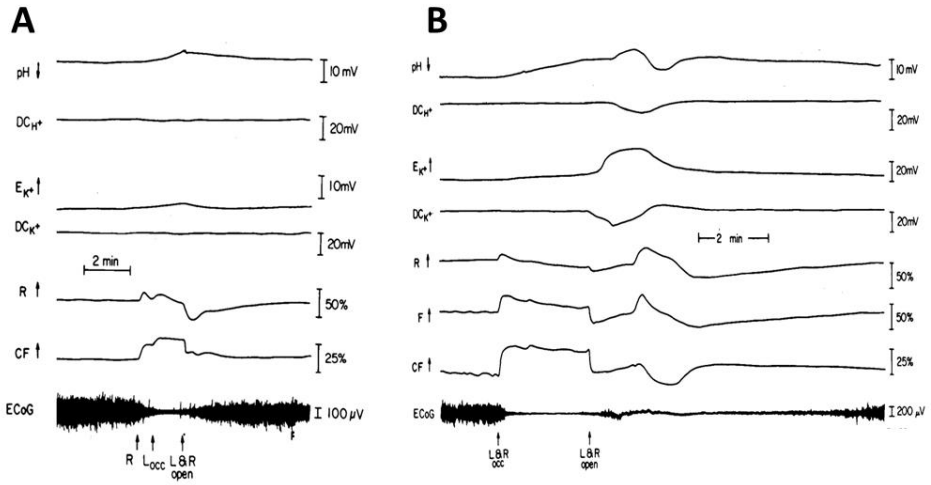

Figure 12: A - Effects of short-term unilateral and bilateral carotid artery occlusion on metabolic ionic and electrical activities in right hemisphere of a gerbil brain. R, Locc, right and left carotid occlusion; L & R open, reopening of two carotid arteries; ECoG, electrocorticogram; CF,corrected fluorescence; R, reflectance; E_{K+}, extracellular K^+ level; DC_{H+}, DC_{K^+}, DC steady potential measured near pH electrode, K^+ electrode, respectively. Arrows, increase in parameters measured.
B - Appearance of a cortical spreading depression phenomenon after short term complete ischemia. After reopening of left and right carotids E_{K+} increased, and NADH (CF) showed an oxidation cycle. Uncorrected fluorescence signal (F) was also recorded instead of DC_F recorded in other figures. Abbreviations as in A [64].

In the last example presented in Figure 13 [39] we added the monitoring of CBF by laser Doppler flowmeter. In this gerbil, the occlusion of the 2 carotid arteries led to severe decrease of CBF (LD_F) and the ID was recorded during the ischemic episode as seen in all monitored parameters. The blood volume (LD_V) also decreased significantly during the ID event as seen also by the increase in the reflectance trace (line A).

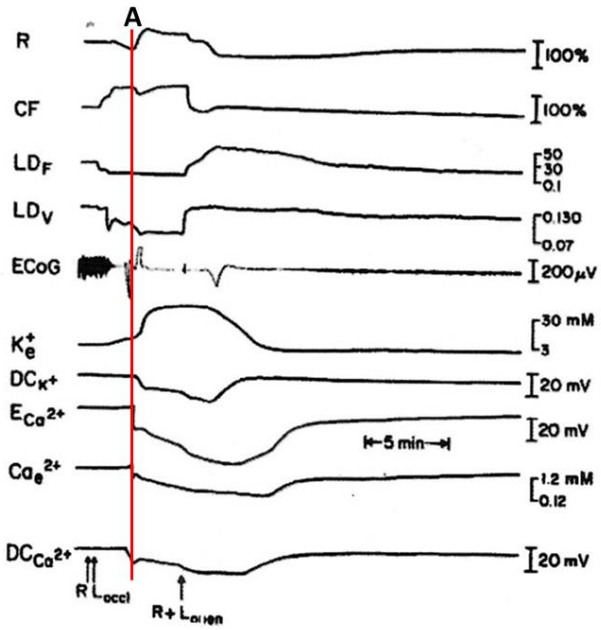

Figure 13: Responses of blood flow and volume as well as other metabolic and ionic parameters to bilateral carotid artery occlusion in the gerbil brain. The light guide of the Laser Doppler was located inside the MPA as seen in Figure 6. R, F, CF-Reflectance, fluorescence and corrected fluorescence; ECoG - Electrocorticogram; E_{K^+}, $E_{Ca^{2+}}$, Uncorrected and corrected potassium and calcium ion concentrations, respectively; DC_{K+}, DC_{Ca2+} - DC steady potential around the K^+ and Ca^{2+} electrodes [39].

Discussion

The gerbil brain is an excellent model in studying cerebral ischemia (stroke), therefore, we performed the present study in order to answer a few basic questions regarding the on line monitoring of the brain metabolic, ionic and electrical activities during and after ischemia. One of the key events occurring under brain ischemia is the development of the complete depolarization associated with the massive ion shifts as well as vasospasm which may induce secondary damage under incomplete ischemia. In the present study we aimed to understand the factors which may lead to the development of the ischemic depolarization (ID) in the gerbil model. In the short term ischemia, another event namely, the cortical spreading depression – CSD may develop. Our multiparametric monitoring approach is a unique one and enabled us to correlate the ionic changes during the ischemic episode to the level of ischemia created by the unilateral or bilateral carotid artery occlusion in the same brain. The main problem in conducting an on-line *in vivo* monitoring of ion homeostasis experiments is the need for dura mater opening or removal in order to measure extracellular K^+ levels. It seems that the removal of the dura mater itself (if done in a very delicate way) did not damage the brain thanks to the fact that the location of the MPA on the brain and the cementation to the skull closed the brain and protected it from swelling. As concluded by Erecinska and Silver [65], 'under normal conditions, the maintenance of ionic gradients requires 50-60% of the total oxygen consumed of which the major fraction is used by the Na^+,K^+-ATPase'. As indicated in the present study, once the blood supply to the brain was diminished, an immediate accumulation of extracellular K^+ was recorded. The main question was, 'Is this K^+ leakage coupled to the level of energy depletion?' To answer this very basic question under *in vivo* conditions, we compared the two ischemic levels created in the gerbil under unilateral or bilateral carotid artery occlusion. Since our measurements were done in the same animal preparation, we eliminated the effects of the variations between individual gerbils as well as the operation itself. Indeed, the rate of K^+ leakage (slope) was significantly different between the R and R+L occlusion in all groups of gerbils [63].

One of the consequences of the different slopes is the development of the ischemic depolarization (ID) in the various groups. The only groups in which ID was not developed under unilateral occlusion were the groups in which the slope was very mild. The practical meaning of it is that those brains in which under clinical situations the development of ID will be avoided (by drugs for example), the beneficiary effect will be evidently significant [66]. As we indicated in Figure 9A, under partial ischemia the ID developed led to a large increase in the reflected light trace (SRI). Using a photography technique (Shaked and Mayevsky, unpublished data) or the laser Doppler flowmetry approach (Mayevsky, unpublished data) we found that during the SRI event, a large vasoconstriction was noted. This vasoconstriction led to a secondary damage to the brain by decreasing O_2 availabilities as well as a massive depolarization which by itself has a negative effect on the brain.

In our previous work [67], we showed that the Ca antagonist, Nimodipine, delayed the appearance of the ID in gerbils under ischemic conditions. Thus the understanding of the mechanism behind the development of ID has a significant meaning to its prevention by drugs. This concept was discussed also by other groups very recently [68,69]. Once the ID started to develop, the effects of the level of ischemia on the development of phase II was minimal. It seems it is an 'all or none' phenomenon. The same type of phenomenon was found when the effect of ischemia duration was studied. It was found that once the ID developed, the rate of leakage of K^+ was the same. Regarding the recovery processes, it seems that the level of K^+ during the ischemia is not the only factor to determine the time to reach a new K^+ level after the recovery. The time to achieve a complete recovery of K^+e was correlated to the duration of the ischemia. The time to the complete recovery of K^+e was shorter under unilateral occlusion suggesting the various levels of ischemia have the same effect as compared to different durations of the same level of ischemia. In the present study we used repeated ischemic episodes in the same animal and we assumed a minimal residual effect of the previous episodes. Kato et al. [70] showed that repeated ischemia episodes led to morphological damage in the selective vulnerable regions. In our study we tested only the cortical region and only gerbils which showed a complete recovery of all parameters were exposed to another episode. Also, we changed the sequence of the R and R&L occlusion in various animals so that any residual effect was canceled out by the statistical procedure. The level of ischemia was calculated by the changes in the intramitochondrial NADH redox state. This approach is the best one that exists for the real time monitoring and in a separate study we found a very good correlation between the NADH redox state responses and the blood flow monitored by a laser Doppler flowmeter (Mayevsky, unpublished results). Also the cerebrovascular anatomy was tested in the

gerbils and was found to be significantly correlated to the NADH redox state changes under unilateral and bilateral carotid artery occlusion [71]. It seems that the main effects of having the dura mater intact during the measurements are on the parameters that represent the rate of diffusion of K^+ to the electrode area. No damage to the brain was created by removing the dura as indicated by the same baseline K^+ levels in all groups of animals. Therefore, we concluded that removal of the dura will provide a stable and reliable model which is also comparable to other studies when microelectrodes are in use. In conclusion, it seems that the gerbil model could provide significant information regarding the development of ischemic damage and recovery. The removal of the dura did not change the behavior of the system and provided more accurate measures of K^+_e. Since the main event to be further investigated is the mechanism of ID development, we are now using the Ca^{2+} electrode which together with the K^+ electrode and redox state monitoring will provide better understanding of brain mechanisms of ischemia as well as recovery. The combination of the various probes in the MPA and the monitoring in real time of the various parameters open up new possibilities for pharmacological as well as clinical applications.

The results presented in Figure 11 demonstrate very clearly the development of CSD wave (B) immediately after the recovery phase from the ischemic episode (A). In the developed CSD wave the NADH became more oxidized (decreased CF signal) as expected. The same coupling between the short ischemic event and the developed CSD is presented in Figure 12B.

Figure 14 presents the comparison between the complete ischemic depolarization developed under severe ischemia (left side) and the CSD developed after the recovery from Mild ischemia (right side).

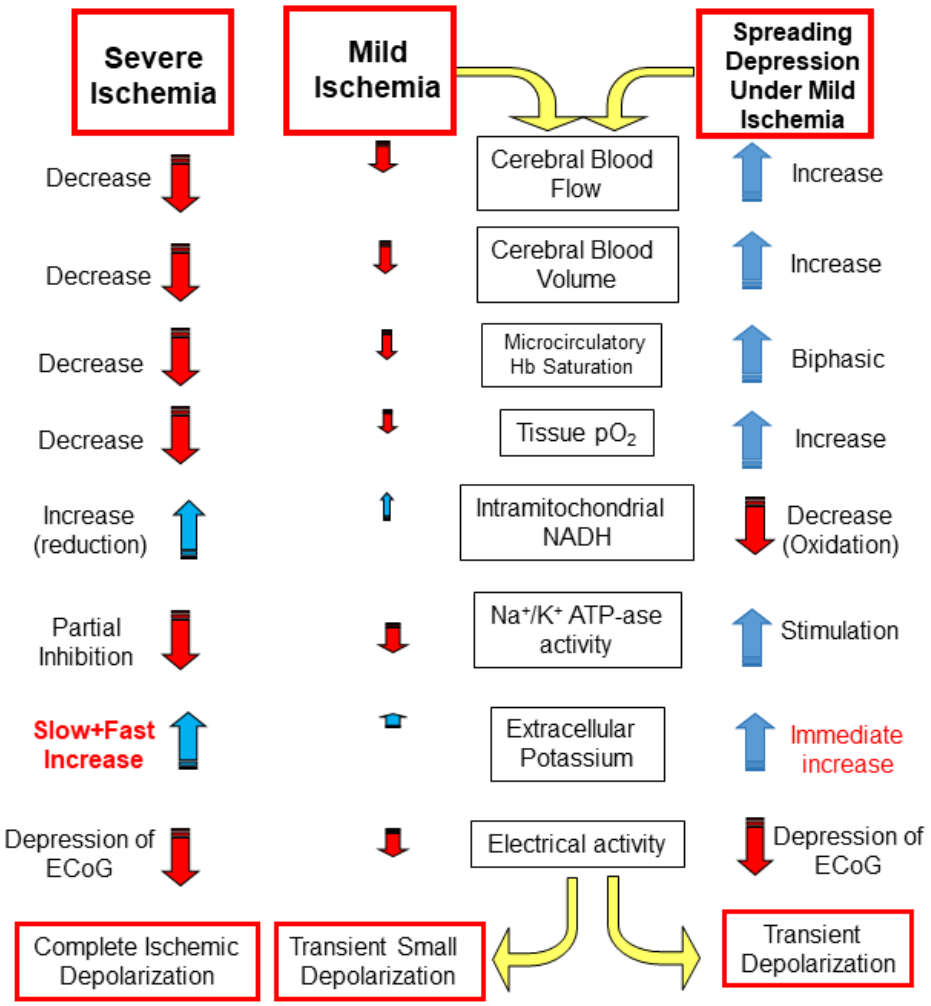

Figure 14: Comparison between sequences of hemodynamics, metabolic, ionic and electrical events developed in the brain under three pathophysiological situations. (modified [50])

In Figure 14, a few of the main events developed during CSD and ischemia were selected and shown in the center column. Under ischemia, the primary event is the decrease in CBF and O_2 delivery to the brain detected as an increase in the intramitochondrial NADH. The next step is the inhibition of the ion pumps such as the Na^+ K^+ ATPase. leading to the accumulation of K^+ in the extracellular space ended up in an ischemic depolarization phase. This situation will persist until the reperfusion started and normal CBF was established.

In CSD, the primary event is the depolarization which propagated in the entire hemisphere. The Na^+ K^+ ATPase is stimulated so that the net accumulation of K^+ in the extracellular space is smaller as compared to ischemia. The large increase in energy utilization will be compensated by the increase in CBF seen in each of the SD waves. Although ischemia and CSD have shared similar ionic disturbances, the differences between the two events are very large. The brain can tolerate CSD waves without any damage created while the damage created under ischemia is well documented

Conclusion

1. The effects of Brain Ischemia (Stroke) on various functions of the brain are dependent on the duration of decreased level in oxygen supply.
2. The accumulation of potassium in the extracellular space is dependent on depletion level in energy supply.
3. During short mild ischemia (2-3 minutes) a wave of Cortical Spreading Depression (CSD) will be initiated.
4. Under moderate or severe ischemia, the event of Ischemic Depolarization(ID) will be recorded.

Conflict of Interest

The author declares that the research was conducted in the absence of any commercial or financial relationships that could be construed as a potential conflict of interest.

Funding Statement

No Funding support.

References

1. Mayevsky A. The 80th Anniversary of Cortical Spreading Depression of Leao: A Major Component in Experimental and Clinical Neuropathology. *Br JHealthcare Med Res*. 2023;10(1):388-408.
2. Barcroft J. *The Respiratory Function of Blood*. Cambridge: Cambridge University Press; 1914.
3. Fink MP. Bench-to-bedside review: Cytopathic hypoxia. *Critical Care (London, England)*. 2002;6:491-499.
4. Robertson CL, Soane L, Siegel ZT, Fiskum G. The potential role of mitochondria in pediatric traumatic brain injury. *Developmental neuroscience*. 2006;28:432-446.
5. Sullivan PG, Krishnamurthy S, Patel SP, Pandya JD, Rabchevsky AG. Temporal characterization of mitochondrial bioenergetics after spinal cord injury. *J Neurotrauma*. 2007;24:991-999.
6. Sims NR, Anderson MF. Mitochondrial contributions to tissue damage in stroke. *Neurochem Internat*. 2002;40:511-526.
7. Ying W. NAD^+ and NADH in cellular functions and cell death. *Front Biosci*. 2006;11:3129-3148.
8. Ying W. NAD^+ and NADH in brain functions, brain diseases and brain aging. *Front Biosci*. 2007;12:1863-1888.
9. Kann O, Kovacs R. Mitochondria and neuronal activity. *Am J Physiol Cell Physiol*. 2007;292(2):C641-C657.
10. Edeas M, Weissig V. Targeting mitochondria: Strategies, innovations and challenges The future of medicine will come through mitochondria. *Mitochondrion*. 2013;13(5):389-390.
11. Chance B, Cohen P, Jobsis F, Schoener B. Intracellular oxidation-reduction states *in vivo*. *Science*. 1962;137:499-508.
12. Chance B, Oshino N, Sugano T, Mayevsky A. Basic principles of tissue oxygen determination from mitochondrial signals. *Oxygen Transport to Tissue, Adv Exp Med Biol*. 1973;37A:277-292.
13. Lubbers DW. Optical sensors for clinical monitoring. *Acta Anaesth Scand Suppl*. 1995;39(104):37-54.
14. Chance B, Williams GR. Steady-state of reduced pyridine nucleotides in phosphorylating rat liver mitochondria. *Am Soc Biol Chem*. 1954;13. Abstract 633.
15. Chance B, Williams GR. Respiratory enzymes in oxidative phosphorylation (III- The steady state). *J Biol Chem*. 1955;217:409-427.
16. Chance B, Williams GR. Respiratory enzymes in oxidative phosphorylation (I- Kinetics of oxygen utilization). *J Biol Chem*. 1955;217:383-393.
17. Connelly CM, Chance B. Kinetics of reduced pyridine nucleotides in stimulated frog muscle and nerve. *Am Physiol Soc*. 1954;13(1):29-.
18. Chance B, Jobsis F. Changes in fluorescence in a frog sartorius muscle following a twitch. *Nature*. 1959;184:195-196.
19. Chance B, Cohen P, Jobsis F, Schoener B. Localized fluorometry of oxidation-reduction states of intracellular pyridine nucleotide in brain and kidney cortex of the anesthetized rat. *Science*. 1962;136:325.
20. Chance B, Legallias V, Schoener B. Metabolically linked changes in fluorescence emission spectra of cortex of rat brain, kidney and adrenal gland. *Nature*. 1962;195:1073-1075.
21. Chance B, Schoener B. Correlation of oxidation-reduction changes of intracellular reduced pyridine nucleotide and changes in electro-encephalogram of the rat in anoxia. *Nature*. 1962;195:956-958.
22. Chance B, Schoener B. Control of oxidation-reduction state of NADH in the liver of anesthetized rats. *Symp Regul Enzyme Act Synth Norm Neoplast Tissues Proc*. 1963:169-185.
23. Chance B, Schoener B, Fergusson JJ. *In vivo* induced oxidation by adrenocorticotrophic hormone of reduced pyridine nucleotide in the adrenal cortex of hypophysectomized rats. *Nature*. 1962;195:776-778.
24. Mayevsky A, Chance B. A new long-term method for the measurement of NADH fluorescence in intact rat brain with implanted cannula. In: Bicher HI, Bruley DF, eds. Vol 37A. New York: Plenum Press; 1973:239-244.
25. Mayevsky A. Brain NADH redox state monitored *in vivo* by fiber optic surface fluorometry. *Brain Res Rev*. 1984;7:49-68.
26. Vatov L, Kizner Z, Ruppin E, Meilin S, Manor T, Mayevsky A. Modeling brain energy metabolism and function: A multiparametric monitoring approach. *Bull Math Biol*. 2006;68:275-291.
27. Mayevsky A, Barbiro-Michaely E. Shedding light on mitochondrial function by real time monitoring of NADH fluorescence: I. Basic methodology and animal studies. *J Clin Monit Comp*. 2013;27:1-34.
28. Mayevsky A, Barbiro-Michaely E. Shedding light on mitochondrial function by real time monitoring of NADH fluorescence: II: Human studies. *J Clin Monit Comp*. 2013;27:125-145.

29. Rutkai I, Merdzo I, Wunnava SV, Curtin GT, Katakam PV, Busija DW. Cerebrovascular function and mitochondrial bioenergetics after ischemia-reperfusion in male rats. *J Cereb Blood Flow Metab*. 2019;39(6):1056-1068.
30. Liu F, Lu J, Manaenko A, Tang J, Hu Q. Mitochondria in Ischemic Stroke: New Insight and Implications. *Aging Dis*. 2018;9(5):924-937.
31. Yang JL, Mukda S, Chen SD. Diverse roles of mitochondria in ischemic stroke. *Redox Biol*. 2018;16:263-275.
32. Sperling JA, Sakamuri S, Albuck AL, et al. Measuring Respiration in Isolated Murine Brain Mitochondria: Implications for Mechanistic Stroke Studies. *Neuromolecular Med*. 2019;21(4):493-504.
33. Chen W, Huang J, Hu Y, Khoshnam SE, Sarkaki A. Mitochondrial Transfer as a Therapeutic Strategy Against Ischemic Stroke. *Transl Stroke Res*. 2020;11(6):1214-1228.
34. An H, Zhou B, Ji X. Mitochondrial quality control in acute ischemic stroke. *J Cereb Blood Flow Metab*. 2021;41(12):3157-3170.
35. Yang M, He Y, Deng S, et al. Mitochondrial Quality Control: A Pathophysiological Mechanism and Therapeutic Target for Stroke. *Front Mol Neurosci*. 2021;14:786099.
36. Tian H, Chen X, Liao J, et al. Mitochondrial quality control in stroke: From the mechanisms to therapeutic potentials. *J Cell Mol Med*. 2022;26(4):1000-1012.
37. Mayevsky A, Lebourdais S, Chance B. The interrelation between brain PO_2 and NADH oxidation- reduction state in the gerbil. *J Neurosci Res*. 1980;5:173-182.
38. Friedli CM, Sclarsky DS, Mayevsky A. Multiprobe monitoring of ionic, metabolic, and electrical activities in the awake brain. *Am J Physiol*. 1982;243(3):R462-469.
39. Mayevsky A, Yoles E, Zarchin N, Kaushansky D. Brain vascular ionic and metabolic responses to ischemia in the Mongolian gerbil. *J Basic Clin Physiol Pharmacol*. 1990;1:207-220.
40. Mayevsky A, Rogatsky G. Mitochondrial function *in vivo* evaluated by NADH fluorescence: From animal models to human studies. *Am J Physiol Cell Physiol*. 2007;292:C615-C640.
41. Mayevsky A, Chance B. Intracellular oxidation-reduction state measured *in situ* by a multicannel fiber-optic surface fluorometer. *Science*. 1982;217:537-540.
42. Dirnagl U, Kaplan B, Jacewicz M, Pulsinelli W. Continuous measurement of cerebral cortical blood flow by laser-Doppler flowmetry in a rat stroke model. *J CBF Metab*. 1989;9:589-596.
43. Haberl RL, Heizer ML, Marmarou A, Ellis EF. Laser-Doppler assessment of brain microcirculation: effect of systemic alterations. *Am J Physiol Heart Circ Physiol*. 1989;256:H1247-1254.
44. Wadhwani KC, Rapoport SI, Shepherd AP, Oberg PA. Blood flow in the central and peripheral nervous systems. In: Shephrd AP, Oberg PA, eds. *Laser Doppler Blood Flowmetry* Vol 107. Boston: Kluwer Academic Pub; 1990:265-304.
45. Mayevsky A. Mitochondrial function and energy metabolism in cancer cells: past overview and future perspectives. *Mitochondrion*. 2009;9:165-179.
46. Meirovithz E, Sonn J, Mayevsky A. Effect of hyperbaric oxygenation on brain hemodynamics, hemoglobin oxygenation and mitochondrial NADH. *Brain Res Rev*. 2007;54(2):294-304.
47. Rampil IJ, Litt L, Mayevsky A. Correlated, simultaneous, multiple-wavelength optical monitoring *in vivo* of localized cerebrocortical NADH and brain microvessel hemoglobin oxygen saturation. *J Clin Monit*. 1992;8(3):216-225.
48. Crowe W, Mayevsky A, Mela L. Application of a solid membrane ion selective electrode to *in vivo* measurements. *Am J Physiol*. 1977;233:C56-C60.
49. Mayevsky A. Multiparameter monitoring of the awake brain under hyperbaric oxygenation. *J Appl Physiol*. 1983;54(3):740-748.
50. Mayevsky A. Biochemical and physiological activities of the brain as *in vivo* markers of brain pathology. In: Bernstein EF, Callow AD, Nicolaides AN, Shifrin EG, eds. *Cerebral Revascularization*. Med-Orion Pub.; 1993:51-69.
51. Mayevsky A, Doron A, Manor T, Meilin S, Salame K, Quaknine GE. Repetitive cortical spreading depression cycle development in the human brain: A multiparametric monitoring approach. *J Cereb Blood Flow Metab* 1995;15:534.
52. Meilin S, Rogatsky GG, Thom SR, Zarchin N, Guggenheimer-Furman E, Mayevsky A. Effects of carbon monoxide exposure on the brain may be mediated by nitric oxide. *J Appl Physiol*. 1996;81:1078-1083.
53. Rogatsky GG, Mayevsky A, Zarchin N, Doron A. Continuous multiparametric monitoring of brain activities following fluid-percussion injury

in rats: Preliminary results. *J Basic Clin Physiol Pharmacol*. 1996;7:23-43.
54. Mayevsky A. Ischemia in the brain: The effects of carotid artery ligation and decapitation on the energy state of the awake and anesthetized rat. *Brain Res*. 1978;140:217-230.
55. Mayevsky A, Chance B. Repetitive patterns of metabolic changes during cortical spreading depression of the awake rat. *Brain Res*. 1974;65:529-533.
56. Mayevsky A, Zeuthen T, Chance B. Measurements of extracellular potassium, ECoG and pyridine nucleotide levels during cortical spreading depression in rats. *Brain Res*. 1974;76:347-349.
57. Mayevsky A, Chance B. Metabolic responses of the awake cerebral cortex to anoxia hypoxia spreading depression and epileptiform activity. *Brain Res*. 1975;98:149-165.
58. Rosenthal M, Somjen G. Spreading depression, sustained potential shifts, and metabolic activity of cerebral cortex of cats. *J Neurophysiol*. 1973;36:739-749.
59. Dora E, Zeuthen T. Brain metabolism and ion movements in the brain cortex of the rat during anoxia. In: Kessler M, ed. *Ion and Enzyme Electrodes in Biology and Medicine*. Baltimore: University.Park Press; 1976:294-298.
60. Mayevsky A, Zarchin N, Tannenbaum B. Brain responses to experimental oxygen deficiency in the Mongolian gerbil. *Adv Exp Med Biol*. 1984;180:191-202.
61. Vyskocil F, Kritz N, Bures J. Potassium-selective microelectrodes used for measuring the extracellular brain potassium during spreading depression and anoxic depolarization in rats. *Brain Res*. 1972;39(1):255-259.
62. Hansen AJ. Effect of anoxia on ion distribution in the brain. *Physiol Rev*. 1985;65:101-148.
63. Mayevsky A. Level of ischemia and brain functions in the Mongolian gerbil *in vivo*. *Brain Res*. 1990;524:1-9.
64. Mayevsky A, Friedli CM, Reivich M. Metabolic, ionic and electrical responses of the gerbil brain to ischemia. *Am J Physiol*. 1985;248:R99-R107.
65. Erecinska M, Silver IA. ATP and brain function. *J Cereb Blood Flow Metab*. 1989;9(1):2-19.
66. Heuser D, Guggenberger H. Ionic changes in brain ischaemia and alterations produced by drugs. *Br J Anaesth*. 1985;57(1):23-33.
67. Cohen S, Mayevsky A. Effects of nimodipine on the responses to cerebral ischemia in the Mongolian gerbil. *Adv Exp Med Biol*. 1989;248:429-438.
68. Dierking H, Tegtmeier E, Holler M, Peters TL. Effects of flunarizine, nimodipine, and diphenylhydantoine on K, Ca and DC in the flunarizine, nimodipine, and diphenylhydantoine on hypoxic cortex of the rat brain *in vivo*. *J Cereb Blood Flow Metab*. 1987;7:S 156.
69. Mori K, Iwayama K, Kawano T, Kaminogo M. DC potential and extracellular K^+ and Ca^{2+} at critical levels of brain ischemia in cats. *J Cereb Blood Flow Metab*. 1978;7:s112.
70. Kato H, Nakano S, Kogure K. Repeated innocent ischemia to the brain can injure the selectively vulnerable neurons in the gerbil and the rat. *J Cereb Blood Flow Metabol*. 1989;9:S642.
71. Mayevsky A, Breuer Z. The Mongolian gerbil as a model for cerebral ischemia. In: Schurr A, Rigor BM, eds.: CRC Press; 1990:27-46.